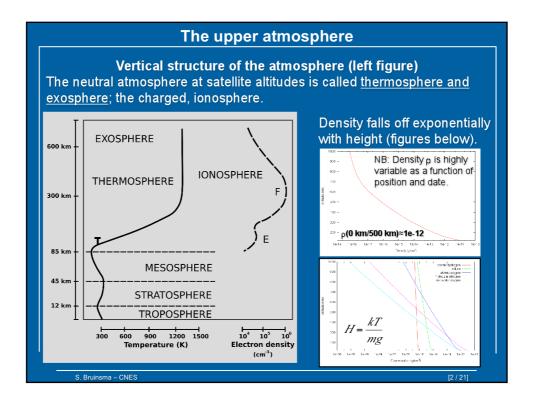


Good afternoon, my name is sean bruinsma. I work at CNES, the french space agency, in the department of terrestrial and planetary geodesy.

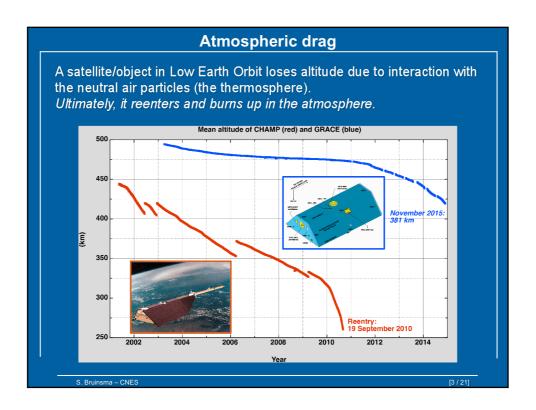
This presentation is on the impact of space weather and space climate on the thermosphere, and specifically the impact on the atmospheric drag as experienced by satellites.



The vertical temperature structure of the atmosphere from the surface to satellite altitudes is shown in the figure on the left. The neutral atmosphere at satellite altitudes of a few hundreds of kilometers minimum is called the thermosphere, and the exosphere for altitudes of 600 km and up. The name thermosphere reflects the temperature profile, which becomes monotonically increasing at about 80-90km, at the mesopause, after which it asymptotically approaches the exospheric temperature. The ionosphere is the ionized component of the upper atmosphere. It plays no role in satellite drag because the concentration of ions is too low, but it has a large impact on the propagation of electromagnetic signals, such as GPS, or satellite altimeters.

[return]

The atmosphere is well mixed up to about 100 km (homosphere), but above that altitude it is gravitationally separated (heterosphere). So a second important property of the thermosphere is that each gas has its own height profile; Heavier gases are major constituents at the lower altitudes of the thermosphere, whereas the lighter gases becomes major constituents at higher altitudes because they decrease more slowly with altitude, as can be seen in the bottom right plot.



Having accurate knowledge of the upper atmosphere density is important in satellite orbit computation because atmospheric drag causes spacecraft in Low Earth Orbit – below about 1500 km altitude – to lose altitude and ultimately to reenter and burn up in the atmosphere. Obviously, we would like to know when this will happen.

This plot shows 2 examples. The first is the satellite CHAMP, which reentered on 19 September 2010, after 10 years in orbit. Notice the 4 orbit raising maneuvers that were necessary to keep the satellite in orbit for 10 years, and not considerably less. To plan such maneuvers, we need to predict the satellite drag, or atmospheric density.

The second example is GRACE, which is orbiting at a higher altitude. No orbit maneuvers were performed, the gaps in the profile are due to days for which I have no data. GRACE is still in orbit, and it was at an altitude of 381 km in November 2015. Notice the changing altitude decay rates. We will later see the reason for this.

Satellite drag acceleration: $a_{drag} = -\frac{1}{2} C_D \frac{A}{m} \rho v^2$ v = satellite speed with respect to co-rotating atmosphere (orbit) A = satellite surface perpendicular to speed, or ram area m = satellite mass $C_D = \text{aerodynamic coefficient } (model)$ $\rho = \text{thermosphere density } (model)$

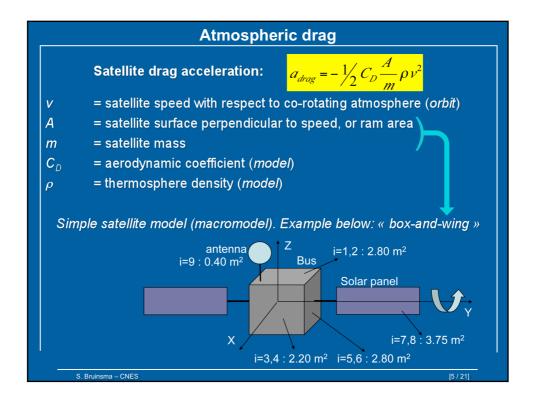
The acceleration due to atmospheric drag on a satellite is given by the equation in the yellow frame.

It depends on parameters that refer to the satellite, such as the surface exposed to drag, the mass as well as the aerodynamic coefficient, which represents the interaction between the satellite walls and the ambient atmosphere or in short the energy transferred from the impinging particles to the satellite.

It also depends on the thermosphere density of course, even if it is extremely low, because of the squared velocity term. Typical satellite speeds in Low Earth Orbit are 7-8 km/s.

[return]

In reality, the drag computation is more complicated because we need a model of the satellite. We use simple shape models, so called macro models, to compute the drag areas. An example of a box-and-wings macro model is given here. For each panel we know the surface and the material. To compute the surface of the panels of the satellite projected on the speed vector v, its attitude must be known, as well as the rotation angle of the solar arrays.



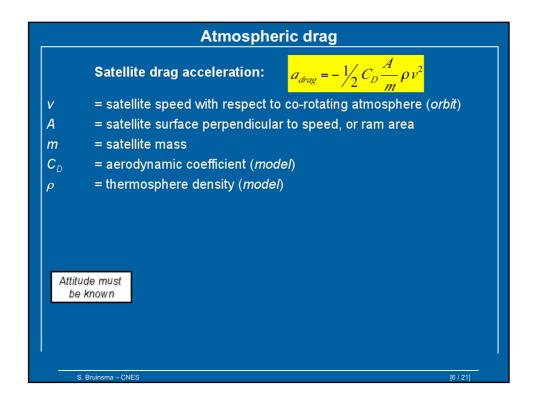
The acceleration due to atmospheric drag on a satellite is given by the equation in the yellow frame.

It depends on parameters that refer to the satellite, such as the surface exposed to drag, the mass as well as the aerodynamic coefficient, which represents the interaction between the satellite walls and the ambient atmosphere or in short the energy transferred from the impinging particles to the satellite.

It also depends on the thermosphere density of course, even if it is extremely low, because of the squared velocity term. Typical satellite speeds in Low Earth Orbit are 7-8 km/s.

[return]

In reality, the drag computation is more complicated because we need a model of the satellite. We use simple shape models, so called macro models, to compute the drag areas. An example of a box-and-wings macro model is given here. For each panel we know the surface and the material. To compute the surface of the panels of the satellite projected on the speed vector v, its attitude must be known, as well as the rotation angle of the solar arrays.



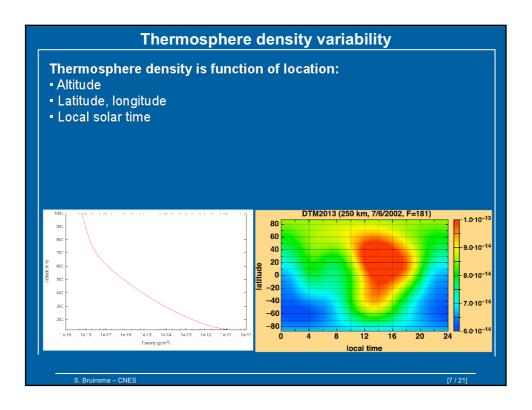
The acceleration due to atmospheric drag on a satellite is given by the equation in the yellow frame.

It depends on parameters that refer to the satellite, such as the surface exposed to drag, the mass as well as the aerodynamic coefficient, which represents the interaction between the satellite walls and the ambient atmosphere or in short the energy transferred from the impinging particles to the satellite.

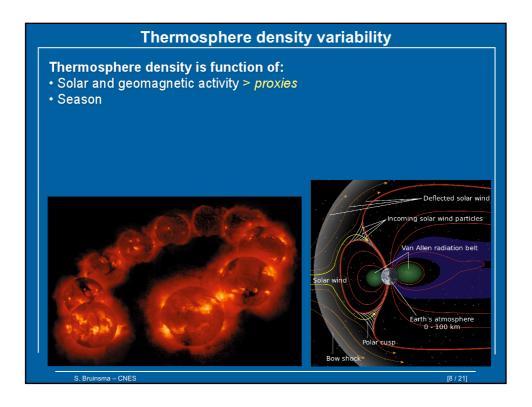
It also depends on the thermosphere density of course, even if it is extremely low, because of the squared velocity term. Typical satellite speeds in Low Earth Orbit are 7-8 km/s.

[return]

In reality, the drag computation is more complicated because we need a model of the satellite. We use simple shape models, so called macro models, to compute the drag areas. An example of a box-and-wings macro model is given here. For each panel we know the surface and the material. To compute the surface of the panels of the satellite projected on the speed vector v, its attitude must be known, as well as the rotation angle of the solar arrays.



Thermosphere density is highly variable, and not only as a function of altitude shown here again on the left. It is also a function of latitude, longitude and local solar time. The plot on the right gives an example of density at 250 km altitude, which clearly shows the "day-night" variation in density: the maximum density lies in the dayside, between 2-3pm local time, and the minimum lies in the nightside. Also clearly visible is the latitude gradient from North to South.



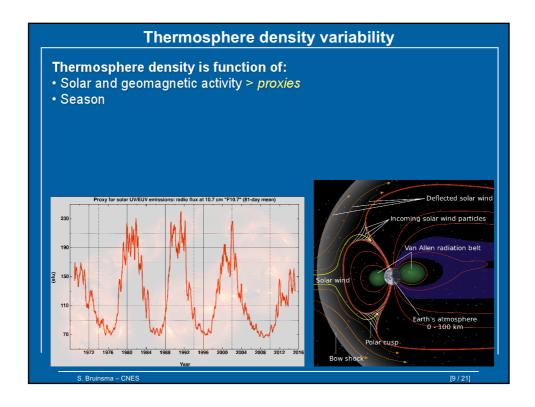
[return]

For that reason, it is called a proxy index, and the solar radio emission at 10.7 cm wavelength is the most common proxy used. It is displayed in this figure for about 4 solar cycles.

A second, even more variable source of intense upper atmosphere heating by currents and particle precipitation is through the interaction of the solar wind with the magnetosphere, which takes place only in the geomagnetic polar caps. This is schematically shown in this figure on the bottom right. The energy deposited at these high latitudes redistributes over the entire earth, but with a delay of several hours at the equator for example. Historically, measurements of the solar wind were not available.

[return]

The common proxy is the planetary averaged perturbation of the geomagnetic field, which is measured by geomagnetic observatories. The right bottom figure presents the daily mean semi-logarithmic Kp index for the year 2003. Notice the peak for 31 October, which was a huge solar storm that I will show later in this presentation again.



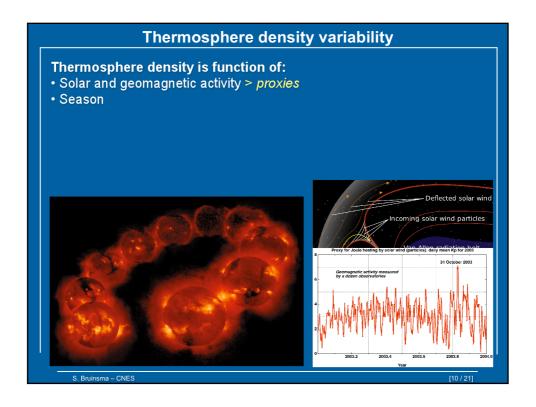
[return]

For that reason, it is called a proxy index, and the solar radio emission at 10.7 cm wavelength is the most common proxy used. It is displayed in this figure for about 4 solar cycles.

A second, even more variable source of intense upper atmosphere heating by currents and particle precipitation is through the interaction of the solar wind with the magnetosphere, which takes place only in the geomagnetic polar caps. This is schematically shown in this figure on the bottom right. The energy deposited at these high latitudes redistributes over the entire earth, but with a delay of several hours at the equator for example. Historically, measurements of the solar wind were not available.

[return]

The common proxy is the planetary averaged perturbation of the geomagnetic field, which is measured by geomagnetic observatories. The right bottom figure presents the daily mean semi-logarithmic Kp index for the year 2003. Notice the peak for 31 October, which was a huge solar storm that I will show later in this presentation again.



[return]

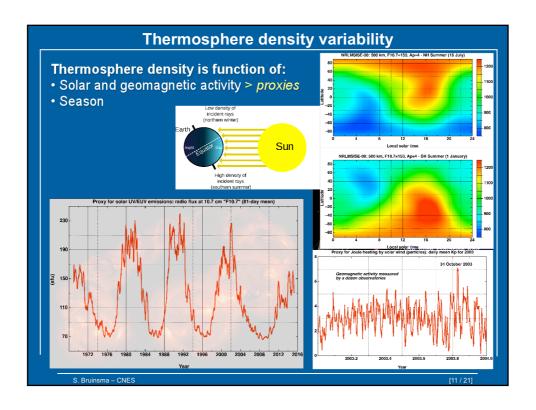
For that reason, it is called a proxy index, and the solar radio emission at 10.7 cm wavelength is the most common proxy used. It is displayed in this figure for about 4 solar cycles.

A second, even more variable source of intense upper atmosphere heating by currents and particle precipitation is through the interaction of the solar wind with the magnetosphere, which takes place only in the geomagnetic polar caps. This is schematically shown in this figure on the bottom right. The energy deposited at these high latitudes redistributes over the entire earth, but with a delay of several hours at the equator for example. Historically, measurements of the solar wind were not available.

[return]

The common proxy is the planetary averaged perturbation of the geomagnetic field, which is measured by geomagnetic observatories. The right bottom figure presents the daily mean semi-logarithmic Kp index for the year 2003. Notice the peak for 31 October, which was a huge solar storm that I will show later in this presentation again.

10



[return]

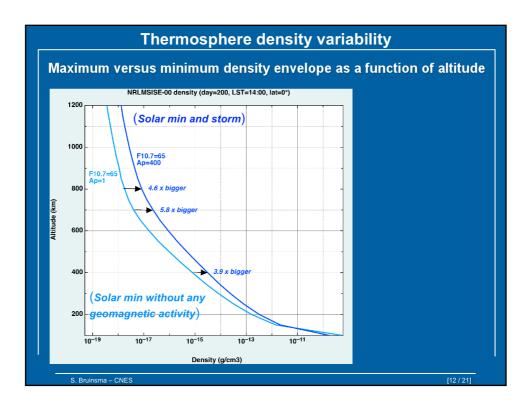
For that reason, it is called a proxy index, and the solar radio emission at 10.7 cm wavelength is the most common proxy used. It is displayed in this figure for about 4 solar cycles.

A second, even more variable source of intense upper atmosphere heating by currents and particle precipitation is through the interaction of the solar wind with the magnetosphere, which takes place only in the geomagnetic polar caps. This is schematically shown in this figure on the bottom right. The energy deposited at these high latitudes redistributes over the entire earth, but with a delay of several hours at the equator for example. Historically, measurements of the solar wind were not available.

[return]

The common proxy is the planetary averaged perturbation of the geomagnetic field, which is measured by geomagnetic observatories. The right bottom figure presents the daily mean semi-logarithmic Kp index for the year 2003. Notice the peak for 31 October, which was a huge solar storm that I will show later in this presentation again.

11



To give an idea of the density variability as a function of altitude due to solar and geomagnetic activity, I have calculated the densities for extreme conditions: a very low solar minimum and no geomagnetic activity, in light blue, and plus an extreme geomagnetic storm of kp=9, in dark blue. The densities are 4-6 times bigger during the storm.

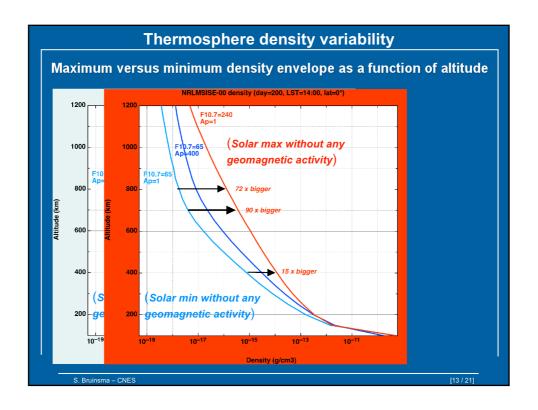
[return]

Now I add the profile for high solar activity, a mean flux of 240, in red. The densities are 15-90 times bigger during the solar cycle maximum in this example.

[return]

And finally I add the profile for high solar activity and an extreme geomagnetic storm, in pink. The densities are 34-275 times bigger for this extreme maximum compared with the extreme minimum.

These are model predictions, in reality storm effects can be larger still.



To give an idea of the density variability as a function of altitude due to solar and geomagnetic activity, I have calculated the densities for extreme conditions: a very low solar minimum and no geomagnetic activity, in light blue, and plus an extreme geomagnetic storm of kp=9, in dark blue. The densities are 4-6 times bigger during the storm.

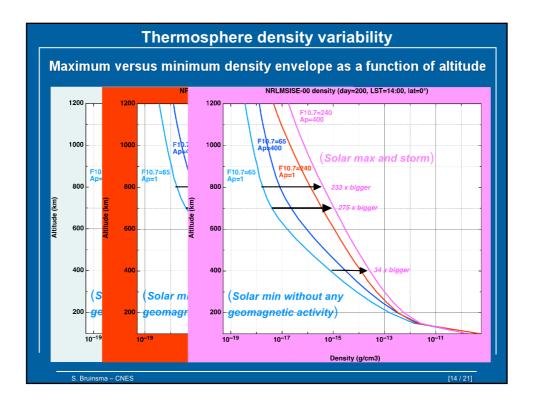
[return]

Now I add the profile for high solar activity, a mean flux of 240, in red. The densities are 15-90 times bigger during the solar cycle maximum in this example.

[return]

And finally I add the profile for high solar activity and an extreme geomagnetic storm, in pink. The densities are 34-275 times bigger for this extreme maximum compared with the extreme minimum.

These are model predictions, in reality storm effects can be larger still.



To give an idea of the density variability as a function of altitude due to solar and geomagnetic activity, I have calculated the densities for extreme conditions: a very low solar minimum and no geomagnetic activity, in light blue, and plus an extreme geomagnetic storm of kp=9, in dark blue. The densities are 4-6 times bigger during the storm.

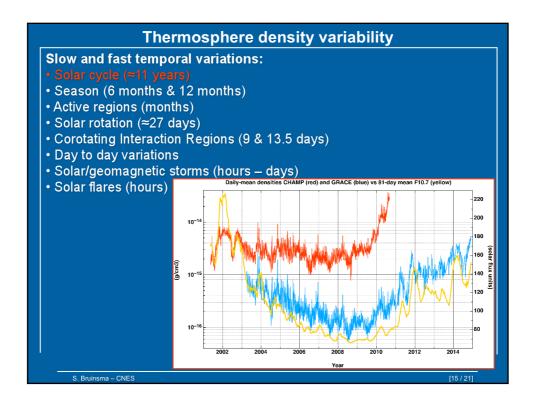
[return]

Now I add the profile for high solar activity, a mean flux of 240, in red. The densities are 15-90 times bigger during the solar cycle maximum in this example.

[return]

And finally I add the profile for high solar activity and an extreme geomagnetic storm, in pink. The densities are 34-275 times bigger for this extreme maximum compared with the extreme minimum.

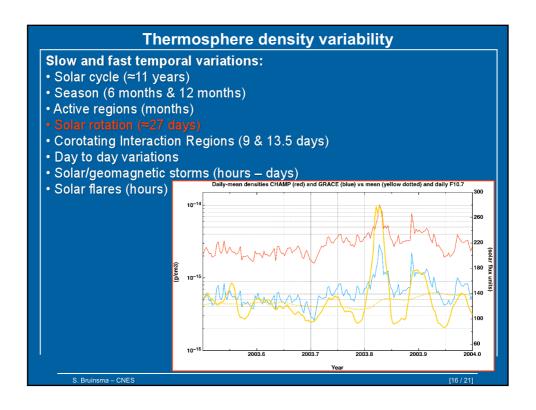
These are model predictions, in reality storm effects can be larger still.



The density variations can be on a long time scale, like the solar cycle of about 11 years, to very short scales of hours or less in case of solar and geomagnetic storms or solar flares. The temporal variations are listed here. I will show some examples of observed variations using densities inferred from the satellites CHAMP and GRACE, the same satellites I showed on slide 3.

This first example illustrates the slow solar cycle variation in density, which is clearly seen in the blue GRACE densities as they follow the mean F10.7 flux in yellow over more than 10 years. The altitude of GRACE did not decrease much over the 7-8 years, which is why the solar activity effect is so clearly visible.

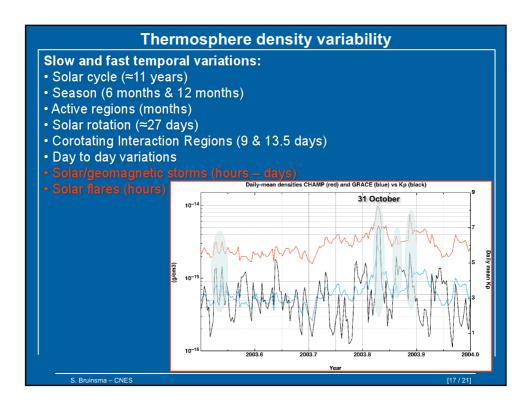
The altitude of CHAMP on the other hand decreased about 100 km from 2001 at solar maximum to 2008 at solar minimum, and this effect approximately equalizes the decreasing solar activity in this case. Density increases fast in the last year due to the rapid orbit decay.



In this second example, the modulation of thermosphere density at the period of the solar rotation of about 27 days is shown. This variation in solar radiation is not always present equally strong, but it was clearly visible in several proxies and emissions in 2003.

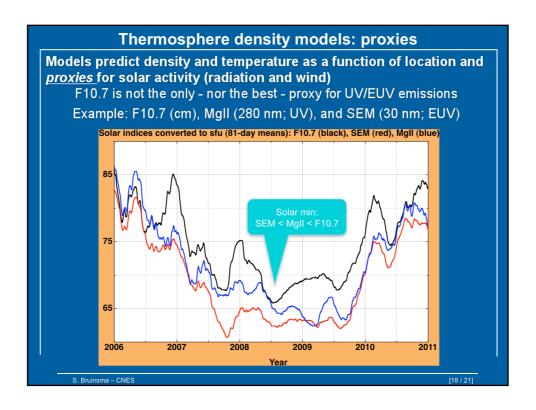
[return]

This figure presents CHAMP and GRACE densities for the second half of 2003, and the mean and daily F10.7 is plotted in yellow. The solar rotation effect is particularly strong at the end of the year, and the densities display the same variation.



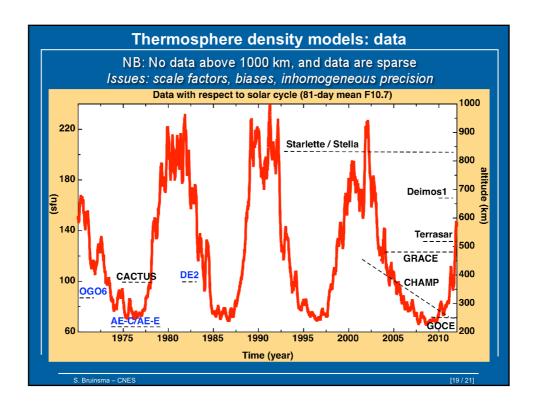
Finally, in this third and last example, CHAMP and GRACE densities are plotted together with the daily mean geomagnetic index Kp in black. [return]

The very large solar storm of 31 October stands out, and we can see that in general the black spikes give rise to spikes in density when storm levels of Kp=5 or higher are reached.



Thermosphere models are not able to reproduce observed densities very precisely for several reasons. An important error is due to the use of a proxy for solar activity, because they do not fully represent the variations in the UV/EUV spectrum. In the past, F10.7 was used exclusively, but starting this century other proxies became available and are used as well. This plot show the MgII index and the SEM Helium II measurement, rescaled to F10.7 units; obviously, these 3 proxies do not display the same variations. If we assume - which is not true - that only one proxy represents the true UV/EUV variation, using one of the other 2 proxies in a model will produce erroneous density variations.

The problem for thermosphere modelers is to decide which proxy, or proxies, to use.



Density and temperature observations in the thermosphere are rather sparse, and this is penalizing especially for the semi-empirical models. The figure illustrates the small number of datasets available as a function of solar activity and altitude on the right axis. Only the blue datasets provide composition and/or temperature observations; none of them is concurrent with high resolution total density observations (after 2000), or with several new solar activity proxies measured with SOHO for example. The new high resolution accelerometer derived densities have only few measurements under high solar maximum conditions. There is less and less data with increasing altitude, and none above 1000 km.

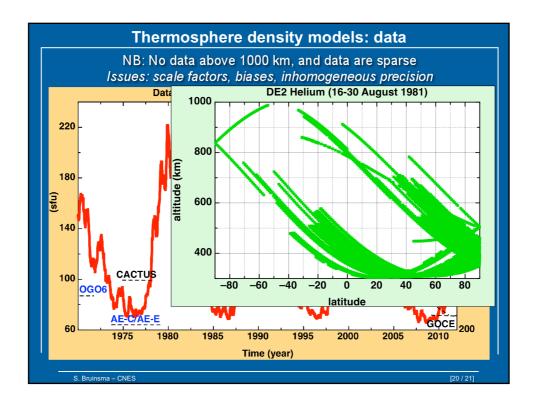
[return]

This figure does not show the poor spatial distribution, an example of which is given here for the Dynamics Explorer 2 Helium measurements. Because of the eccentric orbit of the spacecraft, data are not homogeneously distributed over both hemispheres.

Finally, many datasets have scale errors, some have changing precision over the mission, and the resolution varies from a day to 5 seconds.

[return]

All of the above makes fitting a model to the underlying database difficult. In this example I show the database used in the construction of DTM2013; assimilating different data, or for example applying different scaling factors, will result in different models.



Density and temperature observations in the thermosphere are rather sparse, and this is penalizing especially for the semi-empirical models. The figure illustrates the small number of datasets available as a function of solar activity and altitude on the right axis. Only the blue datasets provide composition and/or temperature observations; none of them is concurrent with high resolution total density observations (after 2000), or with several new solar activity proxies measured with SOHO for example. The new high resolution accelerometer derived densities have only few measurements under high solar maximum conditions. There is less and less data with increasing altitude, and none above 1000 km.

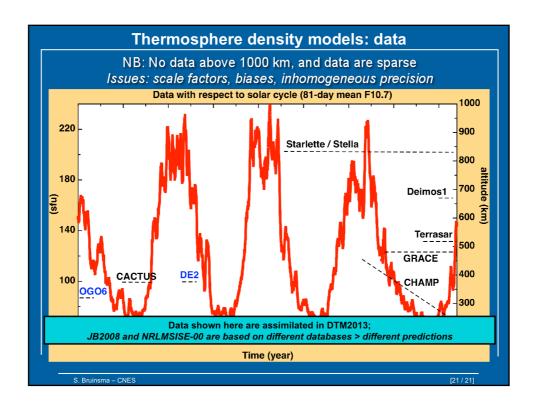
[return]

This figure does not show the poor spatial distribution, an example of which is given here for the Dynamics Explorer 2 Helium measurements. Because of the eccentric orbit of the spacecraft, data are not homogeneously distributed over both hemispheres.

Finally, many datasets have scale errors, some have changing precision over the mission, and the resolution varies from a day to 5 seconds.

[return]

All of the above makes fitting a model to the underlying database difficult. In this example I show the database used in the construction of DTM2013; assimilating different data, or for example applying different scaling factors, will result in different models.



Density and temperature observations in the thermosphere are rather sparse, and this is penalizing especially for the semi-empirical models. The figure illustrates the small number of datasets available as a function of solar activity and altitude on the right axis. Only the blue datasets provide composition and/or temperature observations; none of them is concurrent with high resolution total density observations (after 2000), or with several new solar activity proxies measured with SOHO for example. The new high resolution accelerometer derived densities have only few measurements under high solar maximum conditions. There is less and less data with increasing altitude, and none above 1000 km.

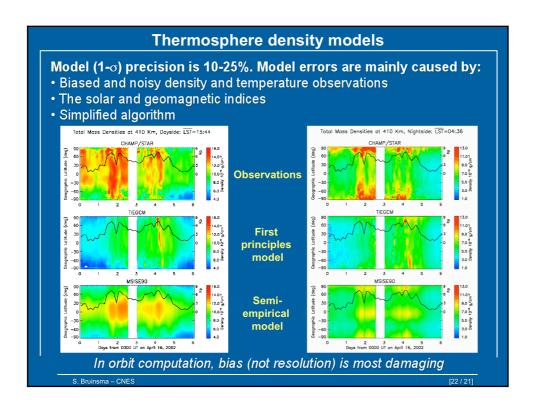
[return]

This figure does not show the poor spatial distribution, an example of which is given here for the Dynamics Explorer 2 Helium measurements. Because of the eccentric orbit of the spacecraft, data are not homogeneously distributed over both hemispheres.

Finally, many datasets have scale errors, some have changing precision over the mission, and the resolution varies from a day to 5 seconds.

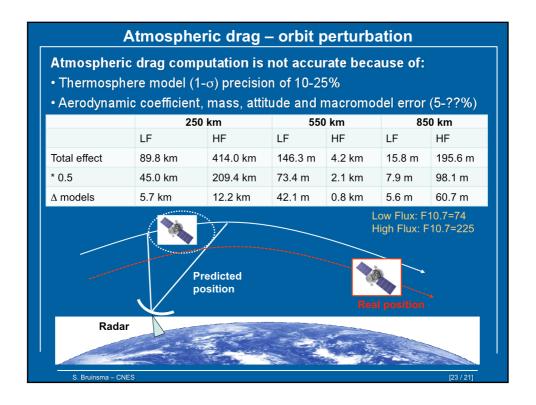
[return]

All of the above makes fitting a model to the underlying database difficult. In this example I show the database used in the construction of DTM2013; assimilating different data, or for example applying different scaling factors, will result in different models.



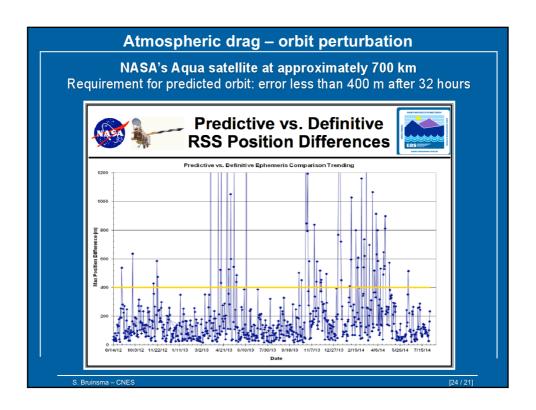
Thermosphere model errors are estimated to 10-25%, 1-sigma, the smallest errors being at low altitude (200-300 km). The model error is due to errors in the assimilated observations, the use of solar and geomagnetic proxies, as well as simplified algorithms. To give an idea of model performance, observed densities are plotted at the top, for dayside on the left and nightside on the right, as a function of latitude and time. The middle frames show the density predicted with a physical model, and the bottom frames with a semi-empirical model. The models significantly underestimate density for this storm. The physical model has higher resolution than the semi-empirical model, but it is also much more biased because it has not assimilated any density data.

Fortunately for orbit computation purposes, the model status is not as poor as it appears. When computing an orbit, the resolution of the thermosphere model is of secondary importance. The orbit error remains relatively small if the average density over a revolution is accurate, it is not necessary to accurately model all bumps and dips visible in the top frames.

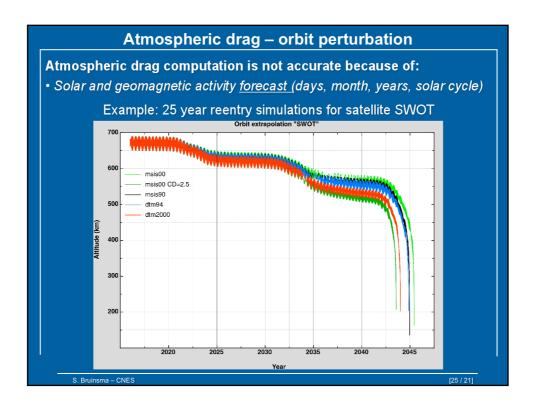


Now let's get back to the satellite drag equation, which was given on slide 4. The thermosphere model error is one of several contributors to the drag model error. The aerodynamic coefficient is often not well-known, and in case of space debris mass and shape are also not accurately known. These errors can all be as large as the thermosphere model error. However, the density model error is not necessarily an offset (the model can be unbiased with a standard deviation of 20%), whereas errors under bullet #2 are. As stated earlier, these systematic errors are most harmful to orbit precision.

The table lists the total in-track position effect of atmospheric drag at 3 altitudes and for low and high solar activity for an imaginary satellite, as well as the effect of a 50% bias. The last line presents the maximum differences between 3 semi-empirical models. At 250 km, the total effect can be hundreds of kilometers, and the error also in worst cases, which can result in failing to acquire the target by a tracking radar. For higher altitudes the errors become much smaller. Notice that the relative model differences are smallest at 250 km, and largest at 850 km.



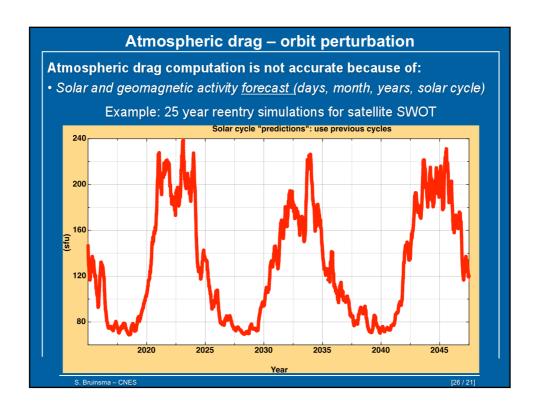
Here is an example of orbit error due to inaccurate drag prediction. The NASA satellite Aqua has a requirement for the error of the predicted orbit, which must not exceed 400 meters after 32 hours. This plot shows that often the requirement is not met, all the dots above the yellow line. These errors are most of the time due to geomagnetic storms that were not predicted – so predicted geomagnetic index kp was small, whereas in reality a geomagnetic storm occurred.



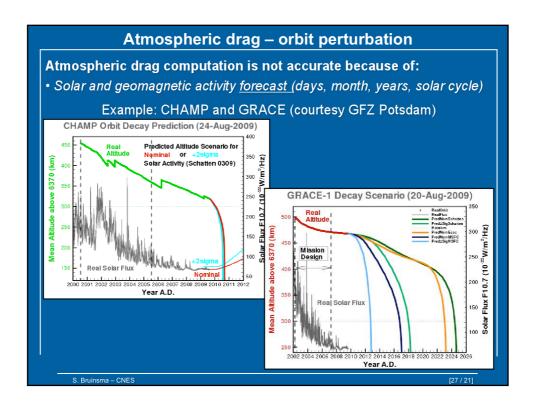
The previous example was over an arc length of 2 days; in this example, a satellite lifetime estimation is shown. This kind of calculation is presently required for satellites to be injected in Low Earth Orbit because the spacecraft reentry within 25 years must be demonstrated.

Here the pure model difference is shown, as well as the effect of using a constant value for the aerodynamic coefficient of 2.5 instead of 2.2. The reentry date varies only by a few years due to model difference in this example.

The main uncertainty of this kind of calculation is due to the solar activity prediction, which is only possible based on statistical methods over such a long period of time.



In the example, I used data from 3 earlier solar cycles; If one or more of the cycles will in reality be weak, such as the present one, the satellite lifetime will be years longer and it will not reenter within 25 years.



Accurate models and solar activity predictions are also necessary for a satellite in operation. For CHAMP for example, the orbit raising maneuvers were necessary at first to achieve the nominal mission, and then to reach the 10 year mark. Once the satellite was below 350 km, the decay accelerated and solar activity predictions did not change the reentry date by more than a month.

[return]

The plot on the right shows the GRACE decay scenario as predicted in August 2009. Several solar activity predictions were used, with very different results. End of 2015, the GRACE altitude was 380 km, which is close to the prediction of NASA's Marshall Space Flight Center in dark blue.

Summary

- Thermosphere variability due to changing energy input, both spatially (season) and temporally (solar activity) orders of magnitude at 700 km
- Models reproduce thermosphere density with a 1- σ precision of 10-25%.
- Improving the models is hampered by:
 - Observations of inhomogeneous quality, sparse data, biases
 - Solar and geomagnetic indices are proxies, with variable performance
- Large uncertainties/errors in atmospheric drag computation
- Largest error on time scale of days: thermosphere model
- Largest error on time scale of months-years: solar activity forecast

S. Bruinsma – CNES [28 / 2